Fluorescence spectra of Cr^{3+} dimers in $LiNbO_3$

Weiyi Jia, Huimin Liu, R. Knutson, and W. M. Yen
Department of Physics, University of Georgia, Athens, Georgia 30602
(Received 7 December 1989)

Fine spectral structure has been observed in both fluorescence and excitation spectra of Cr^{3+}:$LiNbO_3$ on the high-energy side of the broadband emission from $^4T_2$ at 10 K. The lifetimes of the structures are found to be much longer than the lifetime of the broadband $^4T_2$ fluorescence. These sharp lines are assigned to the $^2E \rightarrow {}^4A_2$ emissions (R lines) from two types of Cr^{3+} sites arising from charge compensation; Cr^{3+} ions are found to substitute both for Li^+ and for Nb^{5+} sites and to form dimerlike pairs.

I. INTRODUCTION

The optical properties of transition-metal and rare-earth ions doped in hosts manifesting optical nonlinearity are of interest because of the potential application in various electro-optical and laser technologies. For example, Fan *et al.*[1] have recently reported a new laser based on crystalline $LiNbO_3$:Nd, which exploits the electro-optical and nonlinear-optical properties of the host to make this laser self-Q switch and self-frequency double.

Chromium-doped $LiNbO_3$ crystals possess a strong broadband fluorescence spanning the 770–1170-nm region.[2] This material would add the extra dimension of tunability of the type of laser noted above.

Earlier, Glass[2] conducted a comprehensive study on the absorption and fluorescence spectra of Cr:$LiNbO_3$, and obtained spectral features of Cr^{3+} ions consistent with occupation of low crystal-field sites, i.e., where the $^4T_2$ lies lower than the ^2E. From this, he concluded that Cr^{3+} impurities replaced Nb sites but not the Li sites. However, due to limited range of the excitation light source used in his experiments, a number of ambiguities were raised but left unanswered by this author.

Recently we have analyzed in more detail the spectral structures in the fluorescence and excitation spectra of Cr^{3+} ions in $LiNbO_3$, and have expanded the investigations to include measurement of the lifetimes of both the broadband and sharp line fluorescence. We find that in order to obtain total consistency in the static and dynamic behavior of the spectra, reassignment of the energy levels and reinterpretation of the spectra are required. One of the principal conclusions that can be drawn from our investigation is that Cr^{3+} ions occupy Nb^{5+} and Li^+ sites in such a way as to preserve charge neutrality; the spectra connected with each type of site have been identified.

II. EXPERIMENTAL DETAILS

The Cr^{3+}:$LiNbO_3$ single crystals were grown from the melt by the Czochralski technique. The chromium impurity concentration in the crystal used in this experiment is 0.05 wt. %.

The samples were mounted on a variable temperature refrigerator capable of reaching temperatures as low as 8 K. The 488 nm Ar^+ laser line was used to pump the $^4T_1$ absorption band to produce the Cr^{3+} fluorescence in cw experiments. Site-selective excitation or time-resolved excitation spectral measurements were obtained using a dye laser (LD751) pumped by the frequency doubled output of a yttrium aluminum garnet (YAG) laser. In addition to the LD751 dye laser, a Rhodamine 610 dye laser was also used in order to pump other absorption bands. In these experiments a boxcar, EGG 162/164, was used to sample the signals. The broadband fluorescence was measured by a SPEX single-grating spectrometer and a Varian VMP 159A PMT. All other measurements of emission were obtained using a SPEX 1401 double-grating spectrometer and a cooled RCA C31034 PMT.

III. $^2E \rightarrow {}^4A_2$ TRANSITION AND R LINES

The broadband fluorescence is shown in Fig. 1. At low temperature weak but sharp fluorescence lines are apparent on the higher-energy side of the main fluorescence. Figure 2 shows the behavior of this structure at different temperatures. The temperature dependence of the peak energies are given in Fig. 3. At 10 K the structure consists of three fluorescence lines peaking at 13 615, 13 686, and 13 754 cm^{-1}, and shifting to the red with increasing temperature. At higher temperatures two more lines, peaking at 13 776 and 13 813 cm^{-1}, begin to appear, which shift to the red more rapidly than the low temperature structure as temperature increases.

The α-polarized excitation spectrum (absorption) in the spectral range of interest is shown in Fig. 4 for 10 K. The fluorescence was monitored at 11 700 cm^{-1}. The σ-polarized excitation spectrum is similar to the α spectrum, while the π-polarized spectrum shows the same spectral structure with weaker intensity. It can be seen from Fig. 4 that to within experimental error the excitation energies of the peaks correspond to the energies of the fluorescence lines depicted in Fig. 2. In addition, there is a weak and broader peak at about 13 645 cm^{-1} in the excitation spectrum. This peak arises from a different source than the other features, and will be discussed in detail later.

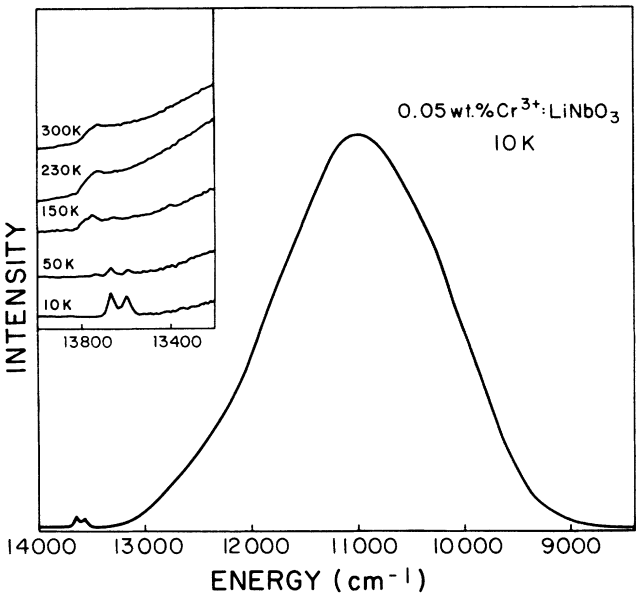

FIG. 1. The broadband fluorescence of the $^4T_2$ state of Cr^{3+} ions in $LiNbO_3$. The fine structure in the inset is identified in the caption of Fig. 2.

In order to assign the spectral structures, we measured the lifetimes of each fluorescence peak. The lifetime of the broadband emission was found to be 10.5 μs at 10 K, while the 13 616- and 13 686-cm^{-1} peaks had lifetimes of 276 and 236 μs respectively. It is obvious from this that the sharp lines are not related to the $^4T_2$ state. The transition at 13 754 cm^{-1} is very weak, and the lifetime could only be estimated to be < 1 μs.

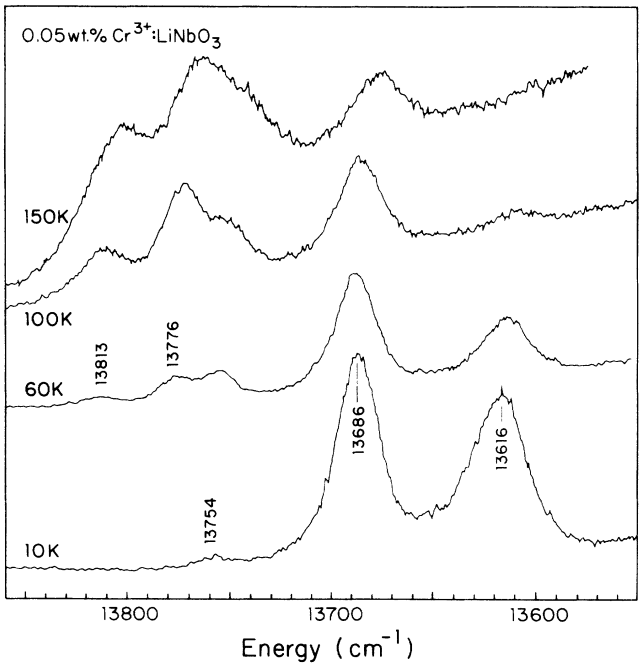

FIG. 2. The fine structures of fluorescence at the high-energy side of the broadband emission of the $^4T_2$ state of Cr^{3+} ions in $LiNbO_3$ at different temperatures. The peaks at 13 616, 13 686, and 13 754 cm^{-1} are assigned to the R_1, R_2+R_1' and R_2' lines of the two sites of Cr^{3+} ions. The peaks at 13 776 and 13 813 cm^{-1} are assigned to the hot phonon satellites of the $^4T_2$ zero-phonon line.

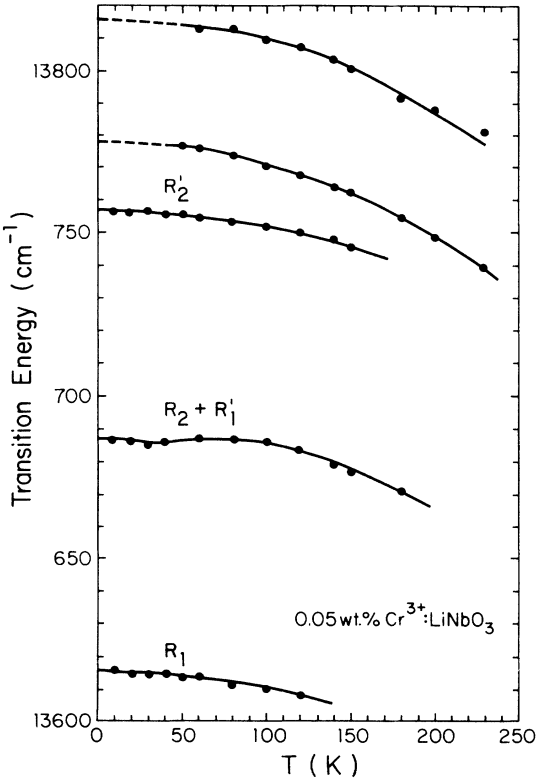

FIG. 3. The temperature dependence of the transition energy of the fluorescence lines shown in Fig. 2.

These results imply that the three fluorescence lines at 13 616, 13 686, and 13 754 cm^{-1} are characteristic of the R lines of the transition $^2E \rightarrow {}^4A_2$. We believe that they originate from Cr^{3+} ions located in different sites, i.e., both at the Nb^{5+} sites and Li^+ sites, forming dimerlike

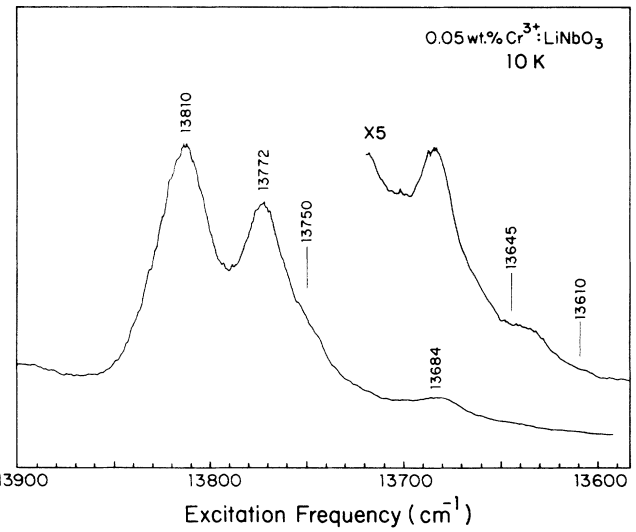

FIG. 4. The uncorrected excitation spectrum of Cr^{3+}:$LiNbO_3$ at 10 K, monitored at 11 700 cm^{-1} and pumped by a LD751 dye laser.

pairs. We denote the lines as R_1, R_2+R_1', and R_2', respectively; R_1 and R_2 are supposed to arise from Cr^{3+}(Nb) ions and R_1' and R_2' from Cr^{3+} in Li sites; R_2 and R_1' are degenerate in energy.

We will provide further experimental evidence to prove the above assignment in the next section. Before that, we would like to discuss the plausibility of our supposition on the basis of the crystal structure.

$LiNbO_3$ is rhombohedral with the space group $R3C$-C_{3v}^6.[3] The Li^+ ions and the Nb^{5+} ions are both situated within the oxygen octahedrons of C_3 symmetry (near C_{3v}), and are distributed alternatively along the C_3 axis of the crystal. There are one or two oxygen layers between neighboring Li and Nb ions. The top and the bottom oxygen triangles of the octahedron are rotated from each other by an angle α. As a result, the C_{3v} symmetry of the octahedron is lowered to C_3 symmetry.[2,3] The sizes of the octahedrons surrounding the Li and Nb ions are nearly the same; the only difference is the extent of the distortion. For the Li octahedrons, $\alpha=3°49'$, while the Nb octahedron has an $\alpha=41'$. In other words, Li situated in a very distorted octahedron. Assuming that the larger distortion gives rise to a higher transition probability for the $^4A_2\rightarrow{}^2E$, then the R_1' and R_2' lines can be tentatively assigned to the Cr^{3+}(Li) ions; thus, the R_1 and R_2 lines may be assigned to the Cr^{3+}(Nb) ions.

Comparing the ionic radii, Li=0.68 Å, Nb^{5+}=0.69 Å, and Cr^{3+}=0.63 Å, and the size of the corresponding octahedrons, the Cr^{3+} ion is as likely to enter the Li^+ sites as the Nb^{5+} sites. On the other hand, the spatial charge will not be compensated if the Cr^{3+} ions substitute exclusively for one or the other anion without interstitial oxygen or oxygen vacancies occurring at the same time. An alternative way to maintain neutrality is for two Cr^{3+} ions to replace simultaneously neighboring Li^+ and Nb^{5+} ions forming a Cr^{3+} pair (dimer). These Cr^{3+} dimers would be oriented along the C_3 axis; in such a case, the crystal-field environment of both Cr^{3+} sites would remain C_3. The similarity of the crystal-field environment for the two sites leads to similar energies for the ^2E and $^4T_2$ states and for the R line splittings as is observed experimentally. The assumption is not without precedent, for example, in doping $Cs^+M^{2+}X_3^-$ compounds (M a metal and X a halide) a pair of Cr^{3+} ions is known to replace three M^{2+} to maintain charge neutrality.[4]

EPR results[5] have shown that all the Cr^{3+} ions are situated in C_3 symmetry sites. However, due to the similar field environments and the broadness of the EPR peaks, the two sites of Cr^{3+} ions could not be resolved. This is in general agreement with our hypothesis above.

IV. SITE-SELECTIVE EXCITATION AND TIME-RESOLVED SPECTRA

Site-selective laser excitation may be employed to resolve the spectra of the individual Cr^{3+} site. Based on the assignment of the energy levels discussed in the next section, the experiment was conducted by pumping the higher-energy side of the 13 813-cm^{-1} peak or the lower-energy side of the 13 776 cm^{-1} resulting in the excitation of the two types of Cr^{3+} sites. Such site-selective excitation spectra are shown in Fig. 5. At pumping frequencies of 13 860 and 13 760 cm^{-1}, the Cr^{3+}(Li) and Cr^{3+}(Nb) ions were excited, respectively, and the R and R' lines were resolved. When the pumping frequency was set at 13 810 cm^{-1}, both of types of the Cr^{3+} ions were excited, and the three fluorescence peaks were observed as in cw excitation case.

The peak 13 686 cm^{-1}, as mentioned above, is the overlap of R_2 and R_1', with the latter dominant. This observation explains the reason why this peak has a long lifetime, and why the relative intensities of the 13 686 and 13 616 cm^{-1} do not follow the Boltzmann rule.[2]

In the dimer model, we have assumed the exchange interaction between Cr^{3+} ion pairs splits the spin degeneracy of the ground state $^4A_2$ and the excited state $\bar{E}+2\bar{A}$.[6,7] The measured linewidths of the R lines are $20(R_1)$, $25(R_2+R_1')$, and $25(R_2')$ cm^{-1}, respectively. It is due to such broadness of the R lines that the exchange splitting is unresolvable.

Figure 6 shows the time-resolved spectra of the R lines. The emission peaks shift to lower energies as a function of delay. The shift may arise from the energy migration in the inhomogeneous sites or from the down-cascade from the upper sublevel to the lower one of the exchange splitting of the ^2E state of the dimers. The latter process seems more likely.

The inhomogeneous linewidth may arise from internal

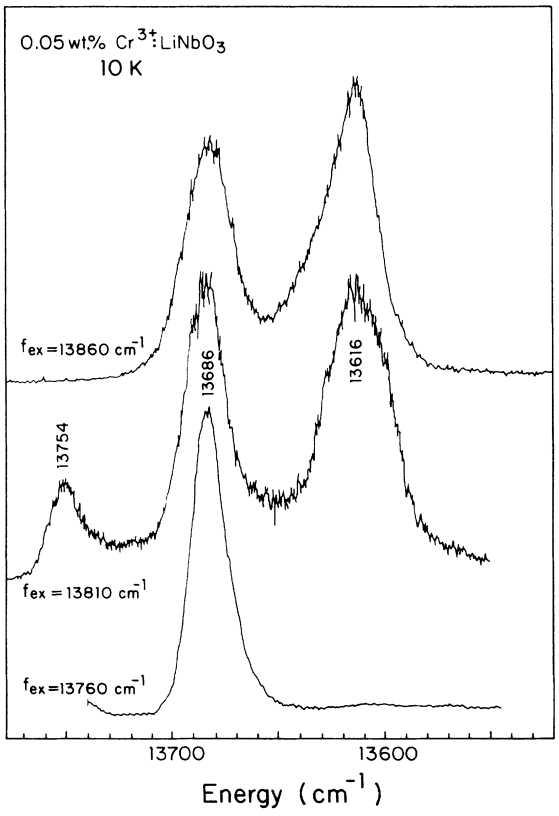

FIG. 5. The site selective excitation spectra of Cr^{3+}:$LiNbO_3$ at 10 K. The excitation energies of the dye laser were set at 13 860, 13 810, and 13 760 cm^{-1} respectively.

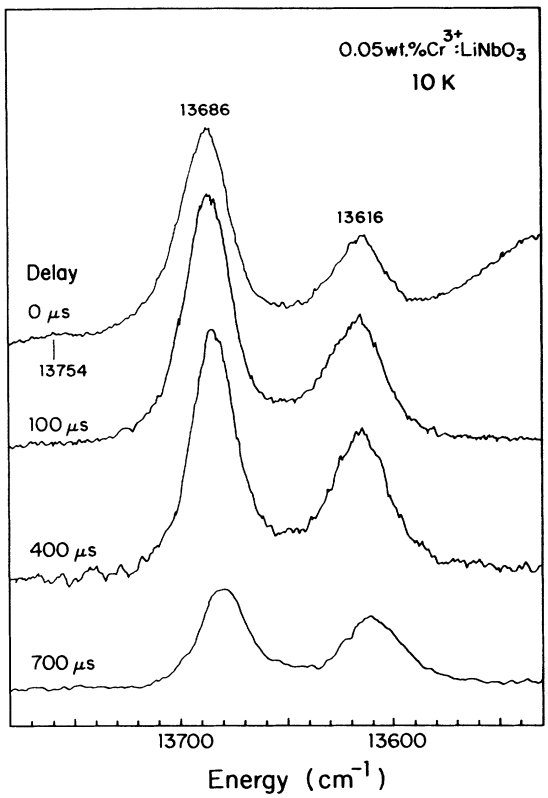

FIG. 6. The time-resolved spectra of the R lines of Cr^{3+}:$LiNbO_3$ at 10 K.

strain, which is inherent usually in charge mismatched substitution and in ferroelectricity with domains. The effect of strain on the linewidth will be enhanced by a large mixing of $^4T_2$ into ^2E in a system[8] such as Cr^{3+}:$LiNbO_3$ where these two energy levels are nearly degenerate.

V. ZERO-PHONON LINES OF THE $^4T_2$ STATE

It is difficult to determine the position of the zero-phonon lines of the $^4T_2$ state of the Cr^{3+} ions in $LiNbO_3$. Glass[2] estimated that the zero-phonon line of $^4T_2$ was below the ^2E state by 400 cm^{-1}. Some theoretical calculations[9] estimated that $^4T_2$ and ^2E are almost degenerate.

From our investigation, the absorption peak at 13 645 cm^{-1} in the excitation spectrum (Fig. 4) is assigned to the zero-phonon line of the $^4T_2$ state. It consists of the zero-phonon lines of both $^4T_2(E)$ and $^4T_2(A)$ with a splitting of less than 30 cm^{-1}, and the 13 813- and 13 776-cm^{-1} peaks are the phonon satellite of the zero-phonon lines of the $^4T_2(E)$ and $^4T_2(A)$ components, respectively. The average energy of the coupling phonon is 140 cm^{-1}. The $^4T_2$ state of the Cr^{3+}(Nb) ions is higher than that of the Cr^{3+}(Li) ions; as a consequence, the R_1 and R_2 lines appear when the higher-energy wing of the 13 813-cm^{-1} peak is pumped.

The weakness of the $^4T_2$ zero-phonon line absorption is due to the strong electron-phonon interaction existing in this state. Such an interaction is also responsible for the very large Stokes' shift—4630 cm^{-1}. The Huang-Rhys factor was estimated to be 6.5.

The $^4T_2$ zero-phonon line emission is too weak to be seen at 10 K. However, with increasing temperature, the two phonon satellites are thermally populated and emit the fluorescences shown in Fig. 2; this hot phonon sideband emission persists up to room temperature as shown in the inset of Fig. 1. At 35 K, the lifetimes of the emission at 13 813 and 13 776 cm^{-1} were found to be $\tau=7$ μs, and were the same as that measured for the broadband fluorescence of the $^4T_2$ state. On the other hand, the lifetimes of the 13 686- and 13 616-cm^{-1} transitions were measured to be 200 μs; these results indicate that these peaks at 13 813 and 13 776 cm^{-1} are neither the R lines as Glass[2] assigned, nor the R lines' phonon sideband, as must be correlated to the $^4T_2$ state. This analysis is similar to the case of Cr^{3+}:TiO_2,[10] where $^4T_2$ is below ^2E and a sharp line is assigned to the $^4T_2$ zero-phonon line since the lifetime of it is the same as that of the $^4T_2$ broad band emission.

In addition, the energy of the $^4T_2$ state of Cr^{3+} ions depends on the crystalline field strength (Dq) much stronger than the ^2E state. Thus, with increasing temperature, the thermal expansion will decrease Dq, and the $^4T_2$ zero-phonon line and its phonon satellites will shift to the lower energy at a greater rate than the R lines as shown in Fig. 3. It is also noted from Fig. 3 that the temperature behavior of the peak at 13 686 cm^{-1} seems unusual, and a slight increase of the energy around 80 K was observed. This result implies that the energy of R_2 must be a little higher than that of R_1'. The emission from the thermally populated R_2 may cause this net increase in the peak energy of $R_1'+R_2$ in the appropriate temperature range.

From our identification of the spectral lines and the ab-

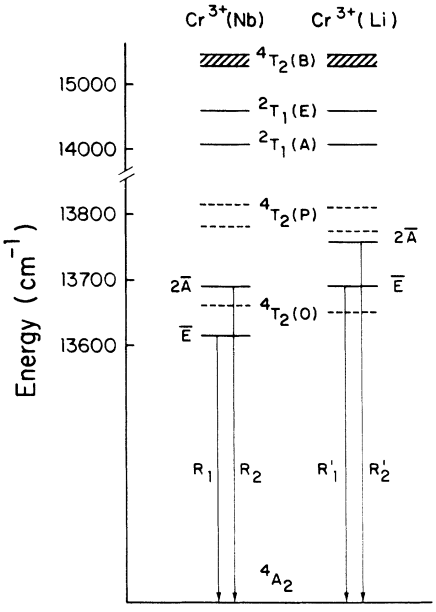

FIG. 7. A tentative energy level scheme of the Cr^{3+} dimers in $LiNbO_3$.

sorption data by Glass,[2] the cubic crystal-field parameter and Racah parameters were recalculated. We obtain: $Dq=1532\ \text{cm}^{-1}$, $B=550\ \text{cm}^{-1}$, $C=2910\ \text{cm}^{-1}$, and $C/B=5.29$. Combined with the ground state splitting, $0.45\ \text{cm}^{-1}$,[4] and the ^2E splitting, $70\ \text{cm}^{-1}$, the on-diagonal trigonal field parameter[11] is found to be $v=-1400\ \text{cm}^{-1}$, while the off-diagonal trigonal field parameter is $v'=700\ \text{cm}^{-1}$. Following Macfarlane,[12] these trigonal field parameters predict a splitting $-700\ \text{cm}^{-1}$ for the $^4T_2$ state, and a splitting approximately $0\ \text{cm}^{-1}$ for the $^4T_1$ state. The absorption data from Glass[2] however show that the splitting of $^4T_2$ is less than $50\ \text{cm}^{-1}$, while the splitting of $^4T_1$ is $540\ \text{cm}^{-1}$. We have no explanation for this discrepancy.

The shape of the broadband fluorescence of the $^4T_2$ state (Fig. 1) seems unusual. A discernible shoulder appears at the high-energy side. It may be the overlapped result of the emissions from the two types of Cr^{3+} sites of dimers.

VI. CONCLUSION

As a summary, a tentative energy level scheme of the Cr^{3+} ion dimers in $LiNbO_3$ is presented in Fig. 7. The dashed lines indicate the zero-phonon lines $^4T_2(0)$ and its single phonon vibronic state $^4T_2(P)$. $^4T_2(B)$ is the broad phonon sideband. It should be noted that the zero-phonon line $^4T_2(0)$ is very close to the R lines. At low temperature, the sharp fluorescence lines from ^2E state were observed. At higher temperature, the emission from the thermally populated $^4T_2(P)$ levels appeared and persisted up to room temperature. Therefore, such a dimer model and its energy level diagram can be used to explain the experimental results quite well.

This work was supported by the National Science Foundation (NSF) under Grant No. DMR-8717696.

[1]T. Y. Fan, A. Gordova-Plaza, and R. L. Byer, in *Spectroscopy of Solid-State Laser-type Materials*, edited by B. Di Bartolo (Plenum Press, New York, 1987), p. 574.
[2]A. M. Glass, J. Chem. Phys. **50**, 1501 (1969).
[3]S. C. Abrahams, J. M. Reddy, and J. L. Bernsten, J. Phys. Chem. Solids **27**, 997 (1966).
[4]P. J. McCarthy and H. U. Gudel, Coord. Chem. Rev. **88**, 69 (1988).
[5]G. Burns, D. F. O'Kane, and R. S. Title, Phys. Lett. **23**, 56 (1966); Phys. Rev. **167**, 314 (1968).
[6]B. G. MacCraith, T. J. Glynn, G. F. Imbusch, J. P. Remeika, and D. L. Wood, Phys. Rev. B **25**, 3572 (1982).
[7]R. C. Powell and B. Di Bartolo, Phys. Status Solidi A **10**, 315 (1972).
[8]C. J. Donnelly, S. M. Healy, T. J. Glynn, G. F. Imbusch, and G. P. Morgan, J. Lumin. **42**, 119 (1988).
[9]F. M. Michel-Calendini, P. Moretti, and H. Chermette, Cryst. Lattice Defects Amorph. Mat. **15**, 65 (1987).
[10]L. Grabner, S. E. Stokowski, and W. S. Brower, Jr., Phys. Rev. B **2**, 590 (1970).
[11]R. M. Macfarlane, J. Chem. Phys. **47**, 2066 (1967).
[12]R. M. Macfarlane, J. Chem. Phys. **39**, 3118 (1963).